

# Synthesis and Characterization of TiO<sub>2</sub>–MgO Mixed Oxides Prepared by the Sol–Gel Method<sup>†</sup>

T. López, J. Hernández, and R. Gómez\*

Department of Chemistry, Universidad Autónoma Metropolitana-Iztapalapa, A.P. 55-534,  
09340 México D. F., Mexico

X. Bokhimi, J. L. Boldú, E. Muñoz, and O. Novaro<sup>‡</sup>

Institute of Physics, The National University of Mexico (UNAM), A.P. 20-364,  
01000 México D. F., Mexico

A. García-Ruiz

UPIICSA, COFAA, The National Polytechnic Institute (IPN), Te No 950 Esq. Resina,  
08400 México D. F., Mexico

Received September 21, 1998. In Final Form: May 14, 1999

Titania–magnesia mixed oxides, with magnesia concentrations between 10 and 90 wt %, were prepared by using the sol–gel method with titanium *n*-butoxide and magnesium ethoxide as precursors. The mixed oxides were characterized with X-ray powder diffraction, BET nitrogen adsorption isotherms, electron spin resonance (ESR), and by testing their catalytic activity for 2-propanol and 2-butanol dehydration. Samples contained periclase, anatase, karooite (MgTi<sub>2</sub>O<sub>5</sub>), geikielite (MgTiO<sub>3</sub>), and qandilite (Mg<sub>2</sub>TiO<sub>4</sub>). The BET specific surface area varied with magnesia concentration; the samples with 50 wt % MgO had the highest area, 211 m<sup>2</sup>/g. Samples had paramagnetic centers that produced complex ESR spectra when many crystalline phases coexisted. For 2-propanol and 2-butanol decomposition, the activity and selectivity patterns of the mixed oxides were substantially different to those observed in pure TiO<sub>2</sub> and pure MgO. This singular behavior should be a result of the structural defects created by the substitution of Mg<sup>2+</sup> ions by Ti<sup>4+</sup> cations in titania lattice, as well as by the interfaces created when several crystalline phases coexisted.

## Introduction

The mixing of solid oxides produces systems that have novel acid or basic properties. Therefore, they are progressively used as catalysts or catalyst supports to replace liquid acids and bases. One advantage of these oxides is that in varying their mixing concentration it is possible to control their acid–base properties. For example, in the MgO–SiO<sub>2</sub> system, which has a basic behavior, its basicity strongly depends on MgO content,<sup>1,2</sup> being maximal for 50 wt % MgO.

In the Al<sub>2</sub>O<sub>3</sub>–SiO<sub>2</sub> mixed oxides, which show an acidic behavior, the acidity has a maximum for 13.0 wt % Al, which is just the highest aluminum concentration that can substitute for silicon in SiO<sub>2</sub>.<sup>3–5</sup> In the TiO<sub>2</sub>–SiO<sub>2</sub> system, the substitution of titanium for silicon in a silica matrix also produces acidity.<sup>6–8</sup> The behavior of ZrO<sub>2</sub>–SiO<sub>2</sub> mixed oxides is different from those mentioned above, because zirconia is not soluble in silica. In this

system, zirconia disperses on a silica surface and gives rise to a basic behavior of the samples.<sup>9–11</sup>

From the above mixed-oxide systems, it is evident that oxide segregation and cation substitution are the main factors that drive acidic–basic properties. When segregation dominates, the oxides do not sinter and preserve unmodified their catalytic properties, but if cation substitution occurs, it determines the catalytic properties.

Because titania and magnesia are important oxides used as catalyst or catalyst supports,<sup>12,13</sup> it is interesting to study the TiO<sub>2</sub>–MgO mixed oxides, which shows a basic behavior.<sup>14</sup> The basicity observed in these materials is attributed to the substitution of titanium ions for magnesium ions in magnesia lattice. This deforms magnesia crystalline structure and produces unbalanced electron charges.

Since the sol–gel method is a good technique to synthesize mixed oxides,<sup>15</sup> we used it to synthesize TiO<sub>2</sub>–MgO samples by co-gelling magnesium ethoxide and titanium *n*-butoxide. Co-gelling metal alkoxides is the best way to obtain a large variety of textures and structures. The bulk characterization of the samples was

\* To whom correspondence should be addressed. E-mail: gomr@xanum.uam.mx. Fax: (52) 5 7244666.

<sup>†</sup> Presented at the Third International Symposium on Effects of Surface Heterogeneity in Adsorption and Catalysis on Solids, held in Poland, August 9–16, 1998.

<sup>‡</sup> Member of El Colegio Nacional, Mexico.

(1) Tanabe, K.; Misono, M.; Ono, Y.; Hattori, H. *New Solid Acid and Bases*; Kodansha: Tokyo, 1989.

(2) Llanos, M. E.; López, T.; Gómez, R. *Langmuir* **1997**, *13*, 974.

(3) Chen, F. R.; Davis, J. G.; Frilat, J. J. *J. Catal.* **1992**, *133*, 263.

(4) Pramanik, P.; Saha, S. K. *J. Mater. Sci. Lett.* **1992**, *11*, 311.

(5) May, M.; Asomoza, M.; López, T.; Gómez, R. *Chem. Mater.* **1997**, *9*, 2395.

(6) Itho, M.; Hattori, H.; Tanabe, K. *J. Catal.* **1974**, *35*, 225.

(7) Ko, E. I.; Chen, J. P.; Weissmann, J. G. *J. Catal.* **1987**, *105*, 511.

(8) Navarrete, J.; López, T.; Gómez, R. *Langmuir* **1996**, *12*, 4385.

(9) Kundu, P.; Pal, D.; Sen, S. *J. Mater. Sci.* **1988**, *23*, 1539.

(10) Acosta, D. R.; Novaro, O.; López, T.; Gómez, R. *J. Mater. Res.* **1995**, *10*, 1397.

(11) Gómez, R.; López, T.; Tzompantzi, F.; Garcíafigueroa, E.; Acosta, D. W.; Novaro, O. *Langmuir* **1997**, *13*, 970.

(12) López, T.; Sánchez, E.; Bosch, P.; Meas, Y.; Gómez, R. *Mater. Chem. Phys.* **1994**, *36*, 222.

(13) López, T.; García, I.; Gómez, R. *J. Catal.* **1991**, *127*, 75.

(14) Tanabe, K.; Hattori, H.; Sumiyoshi, T.; Tanaru, K.; Kondo, T. *J. Catal.* **1978**, *53*, 1.

(15) López, T.; Gómez, R. In *Sol–Gel Optics Processing and Applications*; Klein, L. C., Ed.; Kluwer Academic Publishers: Boston, MA, 1994; p 345.

performed with X-ray powder diffraction and electron spin resonance (ESR). Their surface characterization was done via specific surface BET area and by testing their capability to decompose 2-propanol and 2-butanol.

### Experimental Section

**Catalyst Synthesis.** To a flask with ethanol (150 mL) the appropriate amount of magnesium ethoxide was added to obtain the desired magnesia–titania concentration ratio. Under constant stirring,  $\text{HNO}_3$  was added to this solution to obtain pH 3. Afterward, to complete hydrolysis, 20 mL of water was added, while the solution under reflux was heated to 70 °C. At this temperature, the titanium *n*-butoxide was added drop by drop, and the solution was maintained under reflux and constant stirring until gelling. Gels were dried at 70 °C in air for 12 h. Samples were prepared at  $\text{TiO}_2\text{:MgO}$  weight ratios of 10:90, 50:50, and 90:10. Pure titania and pure magnesia were prepared with the same synthesis conditions. Before characterization, the samples were annealed in air at 400 °C for 12 h.

**Specific Surface Area Analysis.** Specific surface areas were determined on the calcined samples (12 h) with an ASAP-2000 Micromeritics automated apparatus. Pore distributions, and specific surface areas, were calculated from the nitrogen adsorption isotherms, via the BET method.

**X-ray Diffraction Characterization.** Crystalline structures of the calcined samples (12 h) were analyzed with X-ray powder diffraction and refined with the Rietveld method. X-ray diffraction patterns were measured at room temperature in a Siemens D-5000 diffractometer with  $\text{Cu K}\alpha$  radiation. Specimens were prepared by packing sample powder into a glass holder. Intensity was measured by step scanning in the  $2\theta$  range between 10 and 110°, with a step of 0.02° and a measuring time of 2 s per point. For the refinement, DBWS-9411 code was used;<sup>16</sup> a peak profiles model was based on a pseudo-Voigt function that had average crystallite size as a fitting parameter.<sup>17</sup> Standard deviations, showing the variation of numbers last figures, are given in parentheses. When numbers correspond to refined parameters, the standard deviations are not estimates of the analysis as a whole but only of the minimum possible errors based on their normal distribution.<sup>18</sup>

**ESR Characterization.** Before characterization the calcined samples (12 h) were reactivated for 15 min at 400 °C in air. Electron spin resonance experiments were carried out on a JEOL-RE3X spectrometer with a cylindrical cavity ( $\text{TE}_{011}$  mode) operating at X-band frequencies (near 9.15 GHz) and 100 kHz field modulation. *g*-values were obtained by measuring the resonance field with a NMR gaussmeter ES-FC5 (JEOL) and a frequency counter HP-5550B. Spectra were obtained by sweeping the static magnetic field and recording absorption spectrum first derivative.

**Catalytic Activity Evaluation.** Before the activity test the samples were reactivated for 1 h at 400 °C in air. Low conversion tests for 2-propanol and 2-butanol decomposition were performed in a flow reactor coupled to a gas chromatograph, in which the reactants were fed via a saturator with nitrogen as carrier gas. 2-Propanol partial pressure was 22.4 Torr, and that of 2-butanol was only 8.1 Torr. For both decompositions, the nitrogen flow was 3.6 L/h, the reaction temperature was 250 °C, and the catalysts mass was 50 mg. The 2-propanol decomposition produced propene and acetone, and the 2-butanol decomposition produced 1-butene and *cis*- and *trans*-2-butene. The activity values, which had a small dispersion, were obtained by averaging five different measurements with the same flow conditions.

Total reaction rate was calculated from the equation used for flow reactors:

$$(F/22400)(P_{\text{al}}/P_{\text{at}})(273/293)(m)(\%C/100)$$

*F* is reactant flow (mL/s).  $P_{\text{al}}$  and  $P_{\text{at}}$  are the partial pressure of alcohol and atmospheric pressure, respectively, *m* is the catalyst

(16) Young, R. A.; Sakthivel, A.; Moss, T. S.; Paiva-Santos, C. O. *J. Appl. Crystallogr.* **1995**, *28*, 366.

(17) Thompson, P.; Cox, D. E.; Hastings, J. B. *J. Appl. Crystallogr.* **1987**, *20*, 79.

(18) Prince, E. *J. Appl. Crystallogr.* **1981**, *14*, 157.

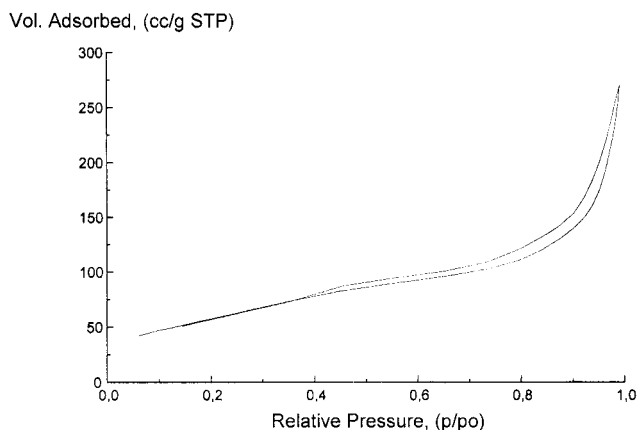


**Figure 1.** Nitrogen adsorption isotherm of the sample with 50 wt % MgO.

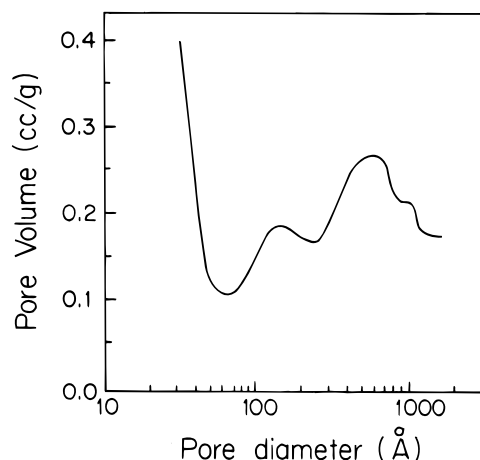


**Figure 2.** Pore size distribution of the sample with 50 wt % MgO.

mass (g), and %C is the total reactant conversion. The selectivity for 2-propanol decomposition was calculated with the following formula:

$$S = \% \text{ mol P1} / \% \text{ mol (P1 + P2)}$$

P1 and P2 are the propene and acetone products, respectively. The selectivity for 2-butanol decomposition was calculated from the formula

$$S = \% \text{ mol P1} / \% \text{ mol (P1 + P2 + P3)}$$

P1, P2, and P3 correspond to 1-butene, *trans*-2-butene, and *cis*-2-butene, respectively.

### Results

**Specific Surface Area.** The nitrogen adsorption isotherm and the pore size distribution of the samples with 50 wt % MgO are shown in Figures 1 and 2, respectively. The isotherm was of type III, while it was of type IV when the samples had 90 wt % magnesia. For both pure titania and pure magnesia, the pore size distribution was monomodal, but that of the mixed oxides was bimodal. Pure titania had a BET area of 111  $\text{m}^2/\text{g}$  (Table 1), which grew when magnesia was added to it and had its maximum value of 211  $\text{m}^2/\text{g}$  for 50 wt % magnesia. The BET area of pure MgO was 115  $\text{m}^2/\text{g}$ . The above large variation of specific areas and mean pore diameters as a function of  $\text{TiO}_2\text{:MgO}$  ratio show that the textural properties of the mixed oxides depend mainly on the relative concentration of their components.

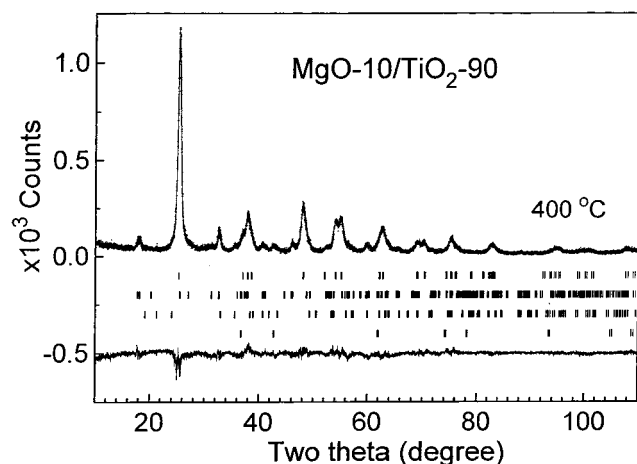


**Figure 3.** Rietveld refinement plot of the sample with 10 wt % magnesia. Crosses represent the experimental data; lines, the calculated diffractogram and its difference with the experimental one. Upper tick marks correspond to anatase, the next down correspond to karooite, the next down correspond to geikielite, and the lowest tick marks correspond to periclase.

**Table 1.** Specific Surface Area and Mean Pore Size Diameter for the Various TiO<sub>2</sub>-MgO Catalysts

catalyst	BET surface area (m <sup>2</sup> /g)	pore diameter (nm)
TiO <sub>2</sub>	111	3.7
TiO <sub>2</sub> :MgO (90:10)	68	(5.5) (12)
TiO <sub>2</sub> :MgO (50:50)	211	(15) (55)
TiO <sub>2</sub> :MgO (10:90)	115	(3.5) (65)
MgO	106	36

**X-ray Diffraction Characterization.** Samples were a mixture of periclase, anatase, Karooite (MgTi<sub>2</sub>O<sub>5</sub>), geikielite (MgTiO<sub>3</sub>), and qandilite (Mg<sub>2</sub>TiO<sub>4</sub>), which differs from Tanabe's et al. report for the same system.<sup>14</sup> They only obtained periclase, anatase, and an amorphous phase.

The concentration of the different crystalline phases and their crystallographic parameters were obtained from the refinement of their structures (Figure 3). The unit cell and symmetry used for anatase, and periclase are published elsewhere.<sup>19,20</sup> Anatase lattice parameter *a* diminished from 0.37838(5) to 0.3756(6) nm when MgO concentration changed from 10 to 50 wt %, while its lattice parameter *c* increased from 0.9481(2) to 0.995(7) nm. Periclase lattice parameter *a* decreased from 0.4238(2) nm for 10.0 wt % MgO to 0.4215(1) for 50 wt % MgO. The values obtained for 50 wt % MgO remained constant at higher magnesia concentrations.

Karooite (MgTi<sub>2</sub>O<sub>5</sub>), which had the same crystalline structure as pseudobrookite (TiFe<sub>2</sub>O<sub>5</sub>), was refined with an orthorhombic unit cell having the symmetry described by space group *Bbmm* and the atom positions published elsewhere.<sup>21</sup> This phase was only present in the samples with 10 wt % magnesia (Table 2), and its lattice parameters were *a* = 0.9732(4), *b* = 0.9973(3) and *c* = 0.3737(1) nm.

Geikielite (MgTiO<sub>3</sub>), the magnesium analogue to ilmenite (FeTiO<sub>3</sub>),<sup>22</sup> was modeled with a trigonal unit cell described by space group *R-3* and the atom positions published elsewhere.<sup>21</sup> This phase appeared only in the

**Table 2.** Phase Concentration (wt %) as a Function of Oxide Composition

sample	anatase	MgTi <sub>2</sub> O <sub>5</sub>	MgTiO <sub>3</sub>	Mg <sub>2</sub> TiO <sub>4</sub>	MgO
TiO <sub>2</sub> :MgO (90:10)	83.8(4)	14.4(4)	1.2(1)		1.5(1)
TiO <sub>2</sub> :MgO (50:50)	0.4(1)		16.1(9)	4.6(6)	78.8(8)
TiO <sub>2</sub> :MgO (10:90)				1.0(1)	99.3(3)

**Table 3.** Average Crystallite Size (nm) as a Function of Oxide Composition

sample	anatase	MgTi <sub>2</sub> O <sub>5</sub>	MgTiO <sub>3</sub>	Mg <sub>2</sub> TiO <sub>4</sub>	MgO
TiO <sub>2</sub> :MgO (90:10)	19(2)	43(4)	62(6)		193(19)
TiO <sub>2</sub> :MgO (50:50)	109(11)		13(1)	8(1)	9(1)
TiO <sub>2</sub> :MgO (10:90)					14.4(4)

samples with 10 and 50 wt % magnesia, and had lattice parameters *a* = 0.5048(3) nm and *c* = 1.3888(8) nm for 10 wt % magnesia and 0.505(2) and 1.341(7) nm for 50 wt %, respectively. In nature, geikielite appears in rutile and spinel minerals.<sup>23</sup>

Qandilite (Mg<sub>2</sub>TiO<sub>4</sub>) was modeled with a spinel structure, which has a cubic unit cell with the symmetry described by space group *Fd3m*. The atom positions for qandilite are published elsewhere.<sup>21</sup> Its lattice parameter *a* varied between 0.8435(3) and 0.848(3) nm. This phase was not found in the samples with low magnesium content.

The samples with 10 wt % magnesia were composed mainly of anatase, but those with 50 wt % contained mainly periclase (78.8 wt %) with only 0.4(1) wt % anatase. The samples with 90 wt % magnesia contained only periclase.

It is well-known that X-ray diffraction sensitivity to detect crystalline phases depends on their concentration and their crystallite size when it is extremely small. A very small crystallite size produces diffraction peaks so wide that the diffraction pattern of its phase, when it appears in a low concentration, can be lost in background. Although, the anatase in the sample with 10 wt % MgO had an average crystallite size of only 19(2) nm (Table 3), its high abundance permitted its analysis.

Periclase average crystallite size depended on the magnesia concentration in the sample (Table 3). When magnesia content was increased, the average crystallite size of MgO notably diminished: It was 193(19) nm for 10 wt % MgO, 9(1) nm for 50 wt % and to 14.4(4) nm for 90 wt % magnesia.

**Electron Spin Resonance Analysis.** The ESR spectra suggest the existence of structural defects in the TiO<sub>2</sub>-MgO mixed oxides (Figure 4). The ESR spectrum of the sample with 10 wt % magnesia had only one absorption peak at 2.0035. When the magnesia content was increased to 50 wt %, the ESR signal became more complex: it had peaks at 2.0090, 2.0085, 2.0057, 2.0035, and 2.0030. The ESR spectrum of the sample with 90 wt % MgO had an absorption peak at 2.0036 and two more peaks with a low intensity at 2.0202 and 2.0091. The complexity of the ESR signal seems to be related to the interaction between the crystalline phases.

**Catalytic Activity Evaluation.** 2-Propanol decomposition is a test reaction that determines the total acidity of a catalyst;<sup>24-25</sup> its products are related to the acidic-basic sites of the catalyst.<sup>26-28</sup> It is currently accepted that the selectivity to propene is an indirect determination of surface acidity, whereas acetone formation involves the

(19) Bokhimi, X.; Morales, A.; Novaro, O.; López, T.; Sánchez, E.; Gómez, R. *J. Mater. Res.* **1995**, *10*, 2788.

(20) Bokhimi, X.; Morales, A.; López, T.; Gómez, R. *J. Solid State Chem.* **1995**, *115*, 411.

(21) Bokhimi, X.; Boldú, J. L.; Muñoz, E.; Novaro, O.; López, T.; Hernández, J.; Gómez, R.; García-Ruiz, A. Submitted for publication in *Chem. Mater.*

(22) Shirane, G.; Pickart, S. J.; Nathans, R.; Ishikawa, T. *J. Phys. Chem. Solids* **1959**, *10*, 35.

(23) Wise, W. S. *Am. Mineral.* **1959**, *10*, 879.

(24) Knonzinger, H. *Adv. Catal.* **1975**, *25*, 184.

(25) DeBoer, J.; Visserer, W. *Catal. Rev.* **1971**, *5*, 55.

(26) Portillo, R.; López, T.; Gómez, R.; Bokhimi, X.; Morales, A.; Novaro, O. *Langmuir* **1996**, *12*, 40.

(27) Szabo, Z.; Jover, B.; Ahmact, R. *J. Catal.* **1975**, *39*, 225.

(28) Ai, A. *Bull. Soc. Chim. Jpn.* **1977**, *50*, 355.



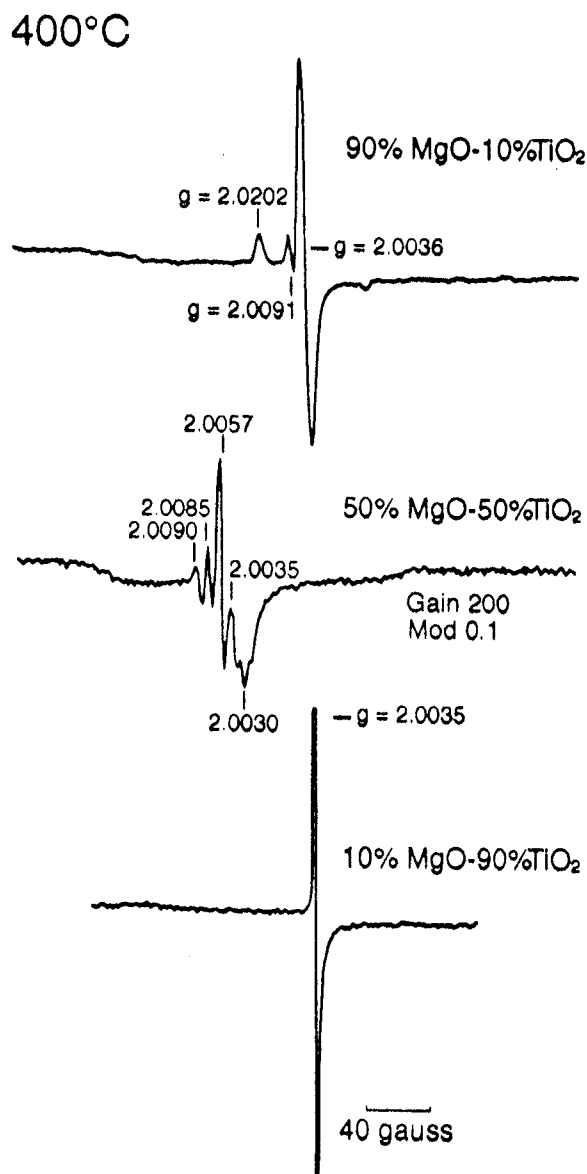


**Figure 4.** ESR spectra of the titania–magnesia oxides for the different magnesium concentrations.

**Table 4.** Selectivity (% mol) and Reaction Rate (mol/(g s)) for the 2-Propanol Decomposition at 250 °C

catalyst	propene	acetone	rate
TiO <sub>2</sub>	100		$3.5 \times 10^{-6}$
TiO <sub>2</sub> :MgO (90:10)	29	71	$3.4 \times 10^{-7}$
TiO <sub>2</sub> :MgO (50:50)	70	30	$8.6 \times 10^{-7}$
TiO <sub>2</sub> :MgO (10:90)	57	43	$6.7 \times 10^{-8}$
MgO	49	51	$3.1 \times 10^{-8}$

presence of both acidic and basic sites. A higher selectivity to acetone will correspond to a higher basicity of the catalyst. The above reaction catalyzed on pure titania produced only propene with a reaction rate 2 orders of magnitude larger than that catalyzed with pure magnesia catalyst (Table 4). The high selectivity to propene in pure TiO<sub>2</sub> is indicative of the acid character of titania. On the other hand, the high concentration of acetone (51%) that formed when the catalyst was pure magnesia confirms its basicity.

The selectivity to acetone of the mixed oxides was different from the one obtained with pure TiO<sub>2</sub> or pure MgO. For example, it was 71% for the sample with 10 wt % magnesia and 51% for pure MgO, but the selectivity to acetone of pure magnesia was larger than the one obtained

**Table 5.** Selectivity (% mol) and Reaction Rate (mol/(g s)) for the 2-Butanol Decomposition at 250 °C

catalyst	1-butene	<i>trans</i> -2-butene	<i>cis</i> -2-butene	rate
TiO <sub>2</sub>	28	19	53	$6.2 \times 10^{-6}$
TiO <sub>2</sub> :MgO (90:10)	26	17	57	$2.0 \times 10^{-6}$
TiO <sub>2</sub> :MgO (50:50)	22	33	45	$9.6 \times 10^{-7}$
TiO <sub>2</sub> :MgO (10:90)	26	29	45	$2.3 \times 10^{-7}$
MgO	25	26	49	$1.7 \times 10^{-7}$

with the samples with 50 wt % titania. The substitution of Mg<sup>2+</sup> ions for Ti<sup>4+</sup> ions in titania lattice gives rise to vacancies, which together with the defects created by the interfacing of the various crystalline phases are expected to be important factors to determine the catalytic properties of the mixed oxides.

The reaction rate and selectivity pattern during 2-butanol decomposition (Table 5) were similar to that described for 2-propanol decomposition. The reaction rate notably diminished when magnesia was added to titania, diminishing also the production of 1-butene but increasing the selectivity to *trans*-2-butene.

### Discussion

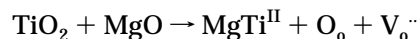
The mixing of titania and magnesia caused a substantial modification of their textural properties when they are pure (Table 1). The textural properties of pure MgO and pure TiO<sub>2</sub> depend on the rate of hydrolysis to condensation reactions. When two alkoxides are co-gelled, the hydrolysis/condensation rates will be modified. Therefore, when titanium and magnesium alkoxides were co-gelled, we expected to have solids with particle size, porosity, and specific surface areas different from those characteristic of the pure oxides. In the MgO–TiO<sub>2</sub> system, the co-gelling of titanium and magnesium alkoxides gave rise to a bimodal pore size distribution.

This co-gelling also affected the specific surface areas, because it modified the lattices of the intermediate phases. The maximum of the specific surface area that was observed in the sample with 50 wt % MgO was evidence of the interactions occurring in the co-gelled oxides.

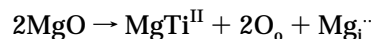
The Rietveld analysis showed that titania-rich samples had a large concentration of anatase, and a large periclase content in magnesia-rich samples. In the samples with 10 wt % magnesia, karooite, geikielite, and qandilite intermediate compounds consumed almost all magnesia; periclase concentration was only 1.5(1) wt %. But in the samples with 50 wt % magnesia, the titania polymorph, anatase, had a concentration of only 0.4(1) wt %.

The above results of the X-ray diffraction analysis correlate well with the complexity of the ESR signals (Figure 4). The ESR spectra of the samples with 50 and 90 wt % magnesia were more complex than those of titania-rich samples, which had only one absorption peak. The structural defects detected by ESR should correspond to large interactions between the crystalline phases.

The most important results of the present work are certainly the activity values obtained for 2-propanol and 2-butanol decomposition. The samples rich in titania have a high selectivity to acetone, but those rich in magnesia have a low selectivity to it. The substitution of Mg<sup>2+</sup> ions for Ti<sup>4+</sup> cations in titania lattice formed structured defects, according to the following equations:



or



Charge neutrality is maintained by Mg interstitials in addition to oxygen vacancies. This changes the acidic and basic properties of the mixed-oxide system in comparison to those of the pure oxides. From Table 2, it is observed that anatase concentration is diminished from 100 wt % in pure titania to 83 wt % when it is mixed with 10 wt % magnesia; anatase became practically undetectable in the samples with 50 wt % MgO. At this magnesia concentration other phases (karooite, geikielite and qandilite) different from anatase were developed. Since the crystalline phases in TiO<sub>2</sub>-MgO catalysts did not correspond to a mixture of anatase and brucite, the expected a selectivity behavior will not correspond to a physical mixture of TiO<sub>2</sub> and MgO. The above results show that co-gelling titania and magnesia alkoxides produce mixed oxides with large activity and selectivity ranges for alcohol decomposition.

### Conclusions

The samples of titania-magnesia mixed oxides prepared via a sol-gel method had a bimodal pore size

distribution, and their crystalline phases were anatase, periclase, karooite, geikielite, and qandilite. The ESR spectra of the samples showed that they have paramagnetic defects in their crystalline phases. The complexity of the spectra suggests that the crystalline phases interact between each other. The selectivity patterns of the mixed oxides did not correspond to a simple addition of those observed for pure TiO<sub>2</sub> and pure MgO. The vacancies created when Mg<sup>2+</sup> ions substitute for Ti<sup>4+</sup> ions and the interaction between the different crystalline structures coexisting in the mixed oxide should be responsible for observed activity and selectivity patterns.

**Acknowledgment.** We acknowledge the support given by the FIES-IMP program and CONACYT Grants. We also thank Mr. A. Morales and Mr. M. Aguilar for technical assistance.

LA9812931